Hydrol. Earth Syst. Sci. Discuss., 7, 5929–5955, 2010
www.hydrol-earth-syst-sci-discuss.net/7/5929/2010/
doi:10.5194/hessd-7-5929-2010

Hydrology and Earth System Sciences Discussions

Soil moisture and evapotranspiration of wetlands vegetation habitats retrieved from satellite images

K. Dabrowska-Zielinska, M. Budzynska, W. Kowalik, and K. Turlej

Institute of Geodesy and Cartography, Remote Sensing Centre, Warsaw, Poland

Received: 22 July 2010 – Accepted: 30 July 2010 – Published: 19 August 2010

Correspondence to: K. Dabrowska-Zielinska (katarzyna.dabrowska-zielinska@igik.edu.pl)

Published by Copernicus Publications on behalf of the European Geosciences Union.

Abstract

The research has been carried out in Biebrza Ramsar Convention test site situated in the N-E part of Poland. Data from optical and microwave satellite images have been analysed and compared to the detailed soil-vegetation ground truth measurements conducted during the satellite overpasses. Satellite data applied for the study include: ENVISAT.ASAR, ENVISAT.MERIS, ALOS.PALSAR, ALOS.AVNIR-2, ALOS.PRISM, TERRA.ASTER, and NOAA.AVHRR. Optical images have been used for classification of wetlands vegetation habitats and vegetation surface roughness expressed by LAI. Also, heat fluxes have been calculated using NOAA.AVHRR data and meteorological data. Microwave images have been used for the assessment of soil moisture. For each of the classified wetlands vegetation habitats the relationship between soil moisture and backscattering coefficient has been examined, and the best combination of microwave variables (wave length, incidence angle, polarization) has been used for mapping and monitoring of soil moisture. The results of this study give possibility to improve models of water cycle over wetlands ecosystems by adding information about soil moisture and surface heat fluxes derived from satellite images. Such information is very essential for better protection of the European sensitive wetland ecosystems.

ENVISAT and ALOS images have been obtained from ESA for AO ID 122 and AOALO.3742 projects.

1 Introduction

The Biebrza National Park is located in Northeast Poland at the border of Western and Eastern Europe. The Park was established in 1993, and with a total area of 59 233 ha it is the largest of the Polish national parks. The Park includes 15 547 ha of forests, 18 182 ha of agricultural land, and 25 494 ha of wetlands, the most valuable habitats of the park. The area of 3936 ha is under strict protection including the Red Bog at the

HESSD

7, 5929–5955, 2010

Forest District. Unique in Europe for its marshes and peat areas, many biodiversity rich plant habitats, as well as its highly diversified fauna, especially birds, the Park was designated as wetland site of global significance as NATURA 2000 and is under the protection of the RAMSAR Convention. Protection and regeneration of wetlands, which are very sensitive ecosystems, are of great importance in ecological research, water cycle, and in nature conservation. The change in water conditions of a given site affects its plant cover. It leads to the elimination or preference of certain species depending on their water needs. Both drying and moorsh-forming (peat degradation) process occurs on a large scale in the Biebrza Valley, mainly due to anthropogenic drainage and fluviogenic feeding limitation. Controlling proper soil moisture content is essential for protection of peat-forming plant communities and slow down drying processes against mineralization. Knowledge of wetlands biophysical properties retrieved from satellite images will enable to improve the monitoring of water cycle of these unique areas, very often impenetrable. The optical data can be used for clear sky conditions and microwave data can also support the overcast conditions.

For the area of Biebrza marshland ecosystem, the method of estimating soil moisture has been presented. To develop the method, various ground truth and satellite data have been used. The satellite images registered in optical spectrum have been classified into different wetlands vegetation classes. For the supervised classification ENVISAT.MERIS data have been used along with the ground truth data. For each of the vegetation classes, the soil moisture was calculated using algorithms developed from ground truth and microwave data. Also, the method of estimating Latent Heat Flux (LE) from NOAA.AVHRR and meteorological data and calculation of soil moisture index as the ratio of Sensible Heat Flux (H) to LE have been presented.

The advantage of using satellite observations is to deliver repetitive information about seasonal and long-term changes of soil moisture, heat fluxes and later evapotranspiration in the sensitive wetland ecosystem. Information about soil moisture and Latent Heat Flux can be used in existing water cycle models to improve their precision and parameters forecasting. The methodology developed is useful for the practitioners dealing

HESSD
7, 5929–5955, 2010

with wetlands ecosystems protection in the other parts of Europe because the studied area can be recognized as a reference for other lowland river valley wetlands.

Sensitivity of radar to water, due to its high dielectric constant, is crucial for examinations of wetlands. Radar wave has been used for differentiate between moist soil and standing water (Kasischke and Bourgeau-Chavez, 1997; Lang et al., 2008). The radar signal is often increased in forested wetlands when standing water is present due to the double-bounce effect (Dwivedi et al., 1999). High sensitivity to surface water and soil moisture makes radar an efficient tool for determining hydropattern (Kasischke et al., 1997a; Rao et al., 1999). It was found that the difference between C-HH band and C-VV band was highly sensitive to flooding (Pope et al., 1997). The studies shows that the radar signals of different frequencies are sensitive to above-ground biomass (Dobson et al., 1992; Le Toan et al., 1992). The combination of L-band using JERS-1 and C-band from RADARSAT increased wetland mapping accuracy (Sahagian and Melack, 1996). Radar data have potential to detect different types of wetlands; it can also be used to study the condition and function of these valuable areas. Recent advances in radar remote sensing data and processing have made the estimation of biomass and other forest parameters possible on a landscape scale (Le Toan, 1992; Kellndorfer, 1998; Kasischke, 1997b). For obtaining biomass of wetlands the ratio of cross-polarized backscattering coefficients (HV or VH) of L- to C-bands has been shown to be well correlated with biomass (Kasischke et al., 1997b). For biomass assessment the combination of different microwave bands and polarizations and optical data were used by Smith (1997). Multi-temporal C-band SAR data C-HH and C-VV from ERS-2 and ENVISAT satellites were used for investigation of inundations and soil moisture determination at wetlands (Lang et al., 2008).

1.1 Test site description

The study has been carried out at the Biebrza Wetlands situated in the Northeast part of Poland and considered as Ramsar Convention Test Site. The geographic location of the test site is between 53°00′ N and 53°50′ N with 22°20′ E and 23°00′ E. Figure 1

HESSD
7, 5929–5955, 2010

presents the area of the Biebrza National Park (test site) on the ALOS.AVNIR-2 RGB (3,2,1) composition. It is one of the largest in Europe natural rich biotope, important zone for nesting and fauna wintering. This area is protected also due to the large amount of unique flora spices. The shrub encroachment, water table lowering, and changes of the farming activity caused ecological problem at these areas. Generally, it is a flat area, the coolest one in Poland with the length of the growing season less than 200 days and mean yearly precipitation less than 500 mm. Summer is warm but short, winter is cold and long. The main river is Biebrza which recipient is Narew River. Biebrza drainage basin area equals to 7051 km^2, river length is 155 km, mean flow amount 35.3 m^3/s.

1.2 Ground truth measurements

Throughout each of the growing seasons and simultaneously to various satellites overpasses the measurements of soil and vegetation parameters were carried out at plots, which were represented by several point measurements chosen for different vegetation habitats. For each of the measurement point geographic coordinates were measured using GPS. Figure 1 presents the boundary of the test site and localization of measured plots on ALOS.AVNIR-2 image. At the test site, the following soil-vegetation parameters have been measured: volumetric soil moisture, SM (with TRIME FM), Leaf Area Index, LAI (with LAI-2000 Plant Canopy Analyser), plant height. The type of vegetation habitat, vegetation development stage and growing conditions were also determined. At the same time, meteorological parameters such as air temperature, wind speed, solar and net radiation, were measured with ENERCO Portable Met Station. All these ground measurements were used along with satellite data in statistical analyses.

1.3 Satellite data

For the present research, the following satellite images have been used: ENVISAT.ASAR (C-band), ENVISAT.MERIS, ALOS.PALSAR (L-band), ALOS.AVNIR-2,

HESSD
7, 5929–5955, 2010

ALOS.PRISM, TERRA.ASTER, and NOAA.AVHRR. Satellite images have been processed using BEST (microwave images), BEAM (optical images) and ERDAS (optical and microwave images) software. Each image has been rectified to the previously geometrically corrected TERRA.ASTER image.

Optical images have been used for wetlands habitats classification and estimation of surface temperature. Sensible Heat (H) flux was calculated using surface temperature determined from NOAA.AVHRR, and meteorological data.

Microwave images have been used for assessment of soil moisture and vegetation parameters. The backscattering coefficient calculated from microwave data represents the integrated respond of several biophysical parameters as soil moisture, surface roughness and vegetation cover. For each of the classified wetland vegetation habitats, the relationship between soil moisture and backscattering coefficient has been examined, and the best combination of microwave variables (wave length, incidence angle, polarization) has been used for soil moisture mapping and monitoring.

2 Application of optical images

Optical satellite images have been used for classification of wetland vegetation habitats and calculation of LAI and heat fluxes. Channels: 2, 5, 7, 8, 10, and 13 of ENVISAT.MERIS, registered on 21 April 2003, have been chosen for supervised classification. Classification has been performed on the pixel-based approach only for wetlands vegetation taken from Corine Land Cover. Figure 2 presents the results of classification as six vegetation classes, which represent the most dominant wetland vegetation habitats: anthropogenic meadows, pastures, sedge-moss, sedge-swamps, reeds, shrubs. Spectral signatures recorded in red and infrared ENVISAT.MERIS channels have been analysed in order to find the best combination for calculation of NDVI, which is correlated with LAI. The best correlation between NDVI and LAI has been found for NDVI calculated with channel 7 (665 nm – chlorophyll absorption) and 13 (865 nm – vegetation discrimination). The obtained values have been compared to those measured

HESSD
7, 5929–5955, 2010

at the test site during the satellite overpass. The mean difference was 6.5%. It was proved that MERIS images could be used to calculate LAI, which was considered as good roughness indicator (Dabrowska-Zielinska et al., 2009). The next step will be application of ALOS.AVNIR-2 and ALOS.PRISM images for classification of wetland vegetation habitats with higher precision (more detailed vegetation communities). Surface temperature (corrected for atmospheric influence) derived from thermal channels of NOAA.AVHRR images in conjunction with meteorological data (air temperature, wind speed, net radiation) have been used for calculation of Sensible Heat Flux (H). Latent Heat Flux (LE) was calculated as a residual of the energy budget equation (Monteith, 1973; Dabrowska-Zielinska et al., 2008). Figures 3–4 show distribution of LE at the test site at the beginning of May 2003 and 2008. It can be noticed that in May 2003 (Fig. 3) values of LE are much lower than in the same period in the year 2008 (Fig. 4). These values reflect ground observations of moisture conditions.

In three considered dates: end of April 2009, beginning of May 2008 and May 2003, quite different vegetation habitats humidity conditions occurred. In May 2008 the Latent Heat Flux was highest from the given cases and exceeded 400 $W\,m^{-2}$ for sedge-moss and pastures. The value for anthropogenic meadows was lower, equal to 300–400 $W\,m^{-2}$. The lowest values occurred on agriculture areas – from 100 to 200 $W\,m^{-2}$. It has to be noted that in May 2008 the conditions were wet. In the same period of the year 2003 soil moisture conditions were much dryer resulting in lower values of LE – the lowest were obtained for shrubs and agriculture areas (100–200 $W\,m^{-2}$). The highest values of LE were noticed in April 2009. For all vegetation classes the lowest values of LE happened in May 2003. In general, among the three considered periods, the values of LE were the highest for May 2008. Taking into account the vegetation habitats, Latent Heat Flux values was the highest for pastures and meadows and the lowest – for shrubs, which occupy dryer sites.

Figure 5 presents correlations between soil moisture (SM) from ground measurements and H/LE index calculated from NOAA.AVHRR and meteorological data. The higher H/LE index the lower SM is.

HESSD
7, 5929–5955, 2010

Soil moisture has been assessed from the Bowen Ratio – ratio of Sensible Heat Flux to Latent Heat Flux (H/LE), (Monteith, 1973), and mapped (Figs. 6–7). High values of soil moisture (SM) are related to low values of the index H/LE, as most of the energy is used to evaporate water and the difference between surface and air temperature ($T_s - T_a$) is low. Often surface temperature is lower than air temperature and Sensible Heat Flux is low. As it can be seen on figures in May 2003 soil moisture conditions were poorer comparing to May 2008, – H/LE index was higher in May 2003 and lower in May 2008. The area of sedge-moss is better distinguished by soil moisture index (H/LE) in the year 2003, when the conditions of arable land were very dry (H/LE>1.5) and the soil moisture index for pastures and meadows was below 1.5. In the year 2008, the conditions were moist and the area of wetlands habitats is not so well distinguished. The values of index H/LE were from 0 up to 1 for agriculture areas and below 0.5 for wetlands meadows. The river valley is not well distinguished.

Application of NOAA.AVHRR data with high temporal resolution for the assessment of Latent Heat Flux and soil moisture proved the possibilities of using this information as the regular input to the water balance of wetlands ecosystem.

3 Application of microwave images

The backscattering coefficient (σ°), calculated from ENVISAT.ASAR and ALOS.PALSAR images represents the integrated respond of soil moisture, surface roughness, and vegetation cover.

Figure 8 presents σ° from ALOS.PALSAR data averaged for classified communities' areas. The differences were caused by various amount of biomass and soil moisture.

There is the influence of vegetation on backscatter of ALOS.PALSAR HH in two ways when the wave penetrates the vegetation to the soil, Fig. 9.

There is the impact of biomass on σ° calculated from ALOS.PALSAR HV, Fig. 10. Biomass for all type of vegetation was higher at 13 June 2009 then at 12 May 2008. However, the correlation of biomass with σ° ALOS.PALSAR HV is rather low.

HESSD
7, 5929–5955, 2010

One of the approaches that have been considered in this research was to present for each of the wetlands vegetation classes (Fig. 2) the relationship between soil moisture (SM) measured at the test site and backscattering coefficient (σ°) calculated from microwave images registered in various modes (IS2, IS4) and polarizations (VV, HV, HH).

Results of the relationship between σ° and SM are described by Dabrowska-Zielinska et al. (2009). The equations, presented there, have been used for the preparation of soil moisture maps. Figures 11–12 present maps of soil moisture for May, 2003 and 2008 calculated using developed algorithms. These maps well describe the moisture conditions – values of SM are higher in May 2008. Similar maps have been produced for each of the ENVISAT.ASAR IS2 HH images.

The impact of LAI and SM on σ° (IS4 VV) was examined in multiple regression – Fig. 13. The coefficients of partial correlations for the independent variables are: for SM 0.76, and for LAI −0.36. It means that SM is in strong positive correlation with σ° ASAR IS4 VV, but LAI has about two times less negative correlation. It was stated that vegetation took part in σ° values when the wave penetrated in two ways vegetation while getting into the soil.

Evapotranspiration depends on amount of water in the root zone and atmospheric conditions but also on vegetation type, and its biomass. There is the relationship between H/LE and ASAR IS4 VV backscattering values for anthropogenic meadows, pastures, sedge-moss, and shrubs, between H/LE and IS4 VH for sedge swamps and between H/LE and IS4 HH for reeds. That shows the dependence of H/LE on vegetation type and moisture. The σ° of IS4 VV is high when H/LE index is low (moist conditions), Fig. 14 shows the relationship between H/LE and σ° IS4 VV for sedge-moss.

Table 1 shows the results of the best relationships between LAI and backscatter as well as between soil moisture (SM) and backscatter obtained applying ALOS.PALSAR.FBD images. The relationship between SM and backscatter has been used for the preparation of SM maps for wetlands communities.

HESSD
7, 5929–5955, 2010

Application of microwave images for the assessment of soil moisture conditions at wetlands areas, very often clouded, was considered as the great possibility for estimation of soil water retention.

4 Conclusions

Taking advantage of multi-mission strategy gives the real possibility of water cycle observations. Exploring the area of one of the largest wetlands in Europe allowed to assess soil moisture, heat fluxes, and evapotranspiration values in the areas of various soil-vegetation conditions and, in many time points, using numerous satellite data. Through classification of satellite optical images (ENVISAT.MERIS) the vegetation habitats covering various wetland areas have been distinguished. The same images have been used for calculation of vegetation indices such as NDVI, which is correlated with LAI. LAI reflects vegetation surface roughness and was used for the assessment of soil moisture from microwave data. Algorithms for soil moisture prediction for each of the vegetation habitats have been developed based on backscattering coefficient from microwave ENVISAT.ASAR (IS2 HH) images. These algorithms have been applied for soil moisture mapping. On the other hand, soil moisture has been assessed from the ratio of Sensible Heat Flux to Latent Heat Flux (H/LE) calculated with surface temperature derived from thermal channels of NOAA.AVHRR images in conjunction with meteorological data. The high similarity was noticed between values of soil moisture obtained from microwave data and soil moisture index H/LE derived from optical data. Comparison of soil moisture maps allows to detect changes in wetlands habitats humidity during one vegetation season or between the different years of observation. Assessed Latent Heat Flux and soil moisture derived from NOAA.AVHRR data could be used as the regular input to the models of water cycle over wetlands ecosystems. Simultaneously, due to the often heavy clouds cover over examined area, results based on microwave data were considered as great possibility for measuring soil-water retention as the input to water balance of wetlands ecosystem.

HESSD
7, 5929–5955, 2010

References

Dabrowska-Zielinska, K., Budzynska, M., Malek, I., Bojanowski, J., Bochenek, Z., and Lewinski, St.: Assessment of crop growth conditions for agri–environment ecosystem for modern landscape management, in: Proceedings of the 28th Symposium of the European Association of Remote Sensing Laboratories: Remote Sensing for a Changing Europe, Istanbul, Turkey, 2–5 June 2008, 247–254, 2008.

Dabrowska-Zielinska, K., Gruszczynska, M., Lewinski, St., Hoscilo, A., and Bojanowski, J.: Application of remote and in situ information to the management of wetlands in Poland, J. Environ. Manage., 90, 2261–2269, doi:10.1016/j.jenvman.2008.02.009, 2009.

Dobson, M. C., Ulaby, F. T., Le Toan, T., Beaudoin, A., Kasischke, E. S., and Christensen, N. C.: Dependence of radar backscatter on conifer forest biomass, IEEE T. Geosci. Remote., 30(2), 412–415, doi:10.1109/36.134090, 1992.

Dwivedi, R. S., Rao, B. R. M., and Bhattacharya, S.: Mapping wetlands of the Sundaban Delta and it's environs using ERS-1 SAR data, Int. J. Remote Sens., 20(11), 2235–2247, doi:10.1080/014311699212227, 1999.

Kasischke, E. and Bourgeau-Chavez, L.: Monitoring South Florida wetlands using ERS-1 SAR imagery, Photogramm. Eng. Rem. S., 63(3), 281–291, 1997.

Kasischke, E., Bourgeau-Chavez, L., Smith, K., Romanowicz, E., and Richardson, C.: Monitoring hydropatterns in South Florida ecosystems using ERS SAR data, Proceedings of the 3rd ERS Symposium on Space at the Service of our Environment, Florence, Italy, 14–21 March 1997, 71–76, 1997a.

Kasischke, E. S., Melack, J. M., and Dobson, M. C.: The use of imaging radars for ecological applications-A review, Rem. Sens. Environ., 59(2), 141–156, doi:10.1016/S0034-4257(96)00148-4, 1997b.

Kellndorfer, J., Pierce, L., Dobson, M., and Ulaby, F.: Toward consistent regional-to-global-scale vegetation characterization using orbital SAR systems, IEEE T. Geosci. Remote., 36(5), 1396–1411, doi:10.1109/36.718844, 1998.

Lang, M. W., Kasischke, E. S., Prince, S. D., and Pittman, K. W.: Assessment of C-band synthetic aperture radar data for mapping and monitoring Coastal Plain forested wetlands in the Mid-Atlantic Region, U.S.A, Rem. Sens. Environ., 112, 4120–4130, doi:10.1016/j.rse.2007.08.026, 2008.

Le Toan, T., Beaudoin, A., Riom, J., and Guyon, D.: Relating forest biomass to SAR data, IEEE

HESSD
7, 5929–5955, 2010

T. Geosci. Remote., 30(2), 403–411, doi:10.1109/36.134089, 1992.
Monteith, J. L.: Principles of environmental physics, edited by: Arnold, E., London, 1973.
Pope, K., Rejmankova, E., Paris, J., and Woodruff, R.: Detecting seasonal flooding cycles in marshes of the Yucatan Peninsula with SIR-C polarimetric radar imagery, Rem. Sens. Environ., 59, 157–166, doi:10.1016/S0034-4257(96)00151-4, 1997.
Rao, B. R. M., Dwivedi, R. S., Kushwaha, S. P. S., Bhattacharya, S. N., Anand, J. B., and Dasgupta, S.: Monitoring the spatial extent of coastal wetlands using ERS-1 SAR data, Int. J. Remote Sens., 20(13), 2509–2517, doi:10.1080/014311699211903, 1999.
Sahagian, D. and Melack, J. (Eds.): Global Wetland Distribution and Functional Characterization: Trace Gases and the Hydrologic Cycle, IGBP Report 46, Report from the Joint GAIM, BAHC, IGBP-DIS, IGAC, and LUCC Workshop Santa Barbara, CA, USA, 16–20 May 1996.
Smith, L. C.: Satellite remote sensing of river inundation area, stage, and discharge: a review, Hydrol. Processes, 11(10), 1427–1439, doi:10.1002/(SICI)1099-1085(199708), 1997.

HESSD
7, 5929–5955, 2010

Table 1. Results of relationships between LAI and backscatter and between soil moisture and backscatter calculated from ALOS.PALSAR.FBD images.

Class	*r*	Equations
Reed and sedge swamps	−0.81	LAI=−0.4–0.2*ALPSR_HV
	0.86	SM=148.3+5.8*ALPSR_ HH
Scrubs and tussock sedge	−0.84	LAI=−5.8–0.5*ALPSR_ HV
	0.89	SM=163.9+8.2*ALPSR_ HH
Sedge-grass	−0.79	LAI=−1.2–0.2*ALPSR_ HV
	0.72	SM=123.5+5.3*ALPSR_ HH
Grass-herb-moss	−0.70	LAI=−1.81–0.26*ALPSR_ HV
	0.73	SM=118.2+4.9ALPSR_ HH
Pastures	−0.71	LAI=−1.9–0.2*ALPSR_ HV
	0.77	SM=153.9+7.8*ALPSR_ HH

HESSD
7, 5929–5955, 2010

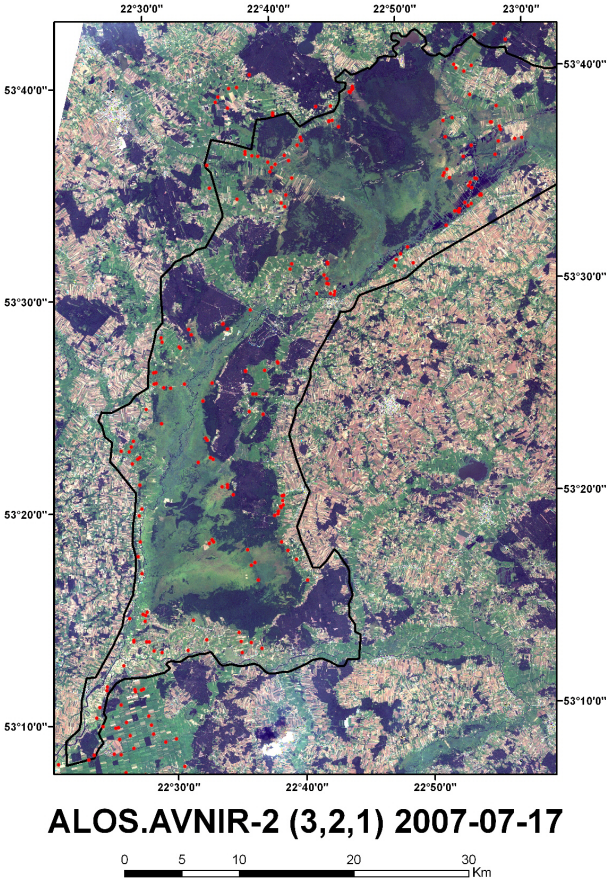

Fig. 1. ALOS.AVNIR-2 image with the test site marked with black curve and measurement plots as red dots.

HESSD
7, 5929–5955, 2010

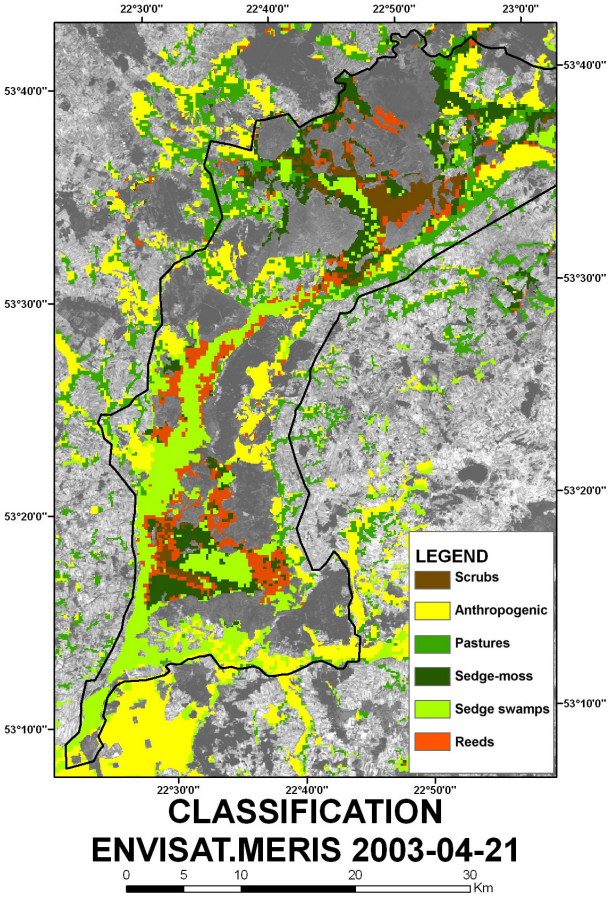

Fig. 2. Classification of wetlands vegetation habitats from MERIS image (first six classes) registered on 21 April 2003.

HESSD
7, 5929–5955, 2010

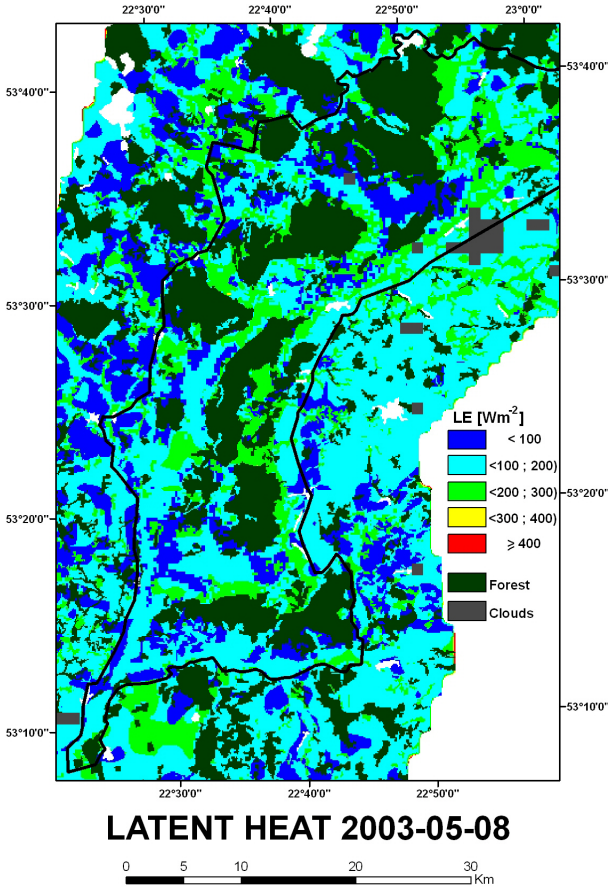

Fig. 3. LE derived from NOAA.AVHRR.

HESSD
7, 5929–5955, 2010

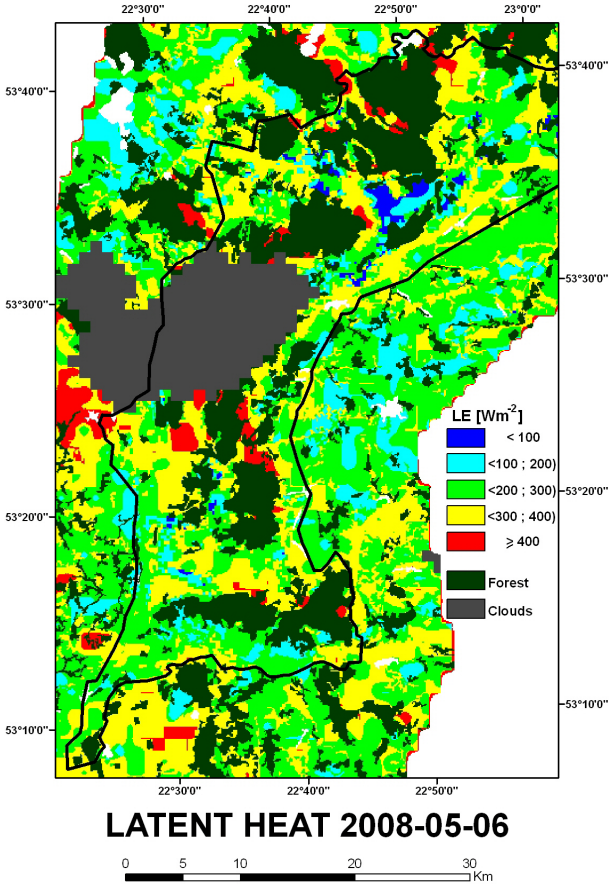

Fig. 4. LE derived from NOAA.AVHRR.

HESSD
7, 5929–5955, 2010

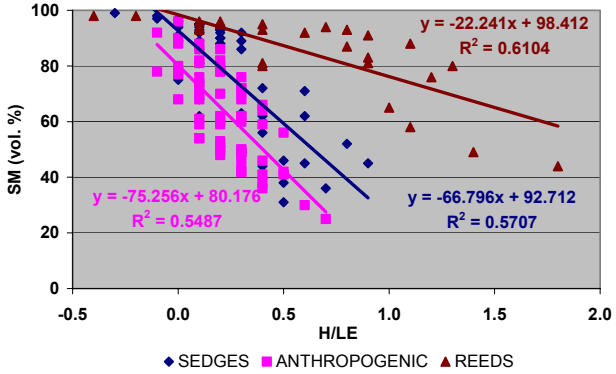

Fig. 5. Relationships between SM and H/LE.

HESSD
7, 5929–5955, 2010

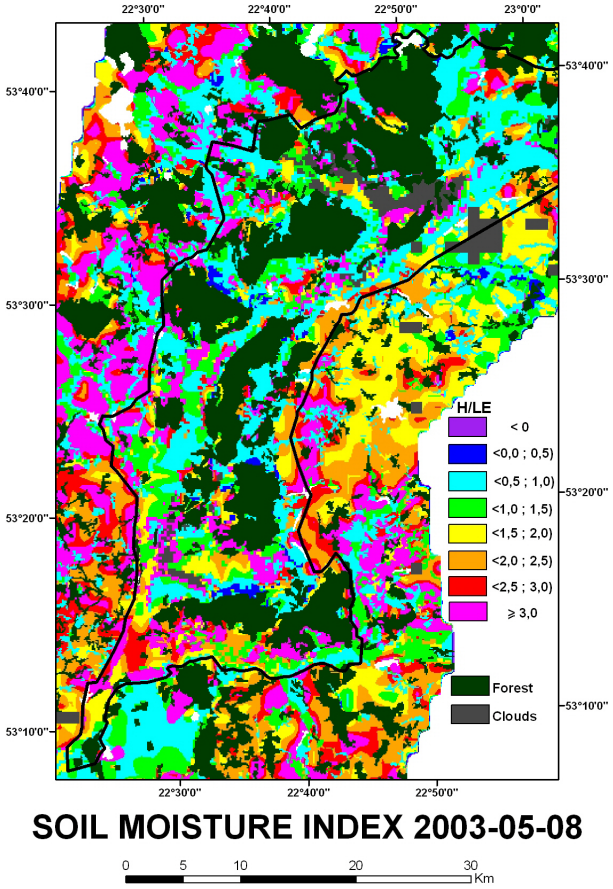

Fig. 6. SM index derived from NOAA.AVHRR.

HESSD
7, 5929–5955, 2010

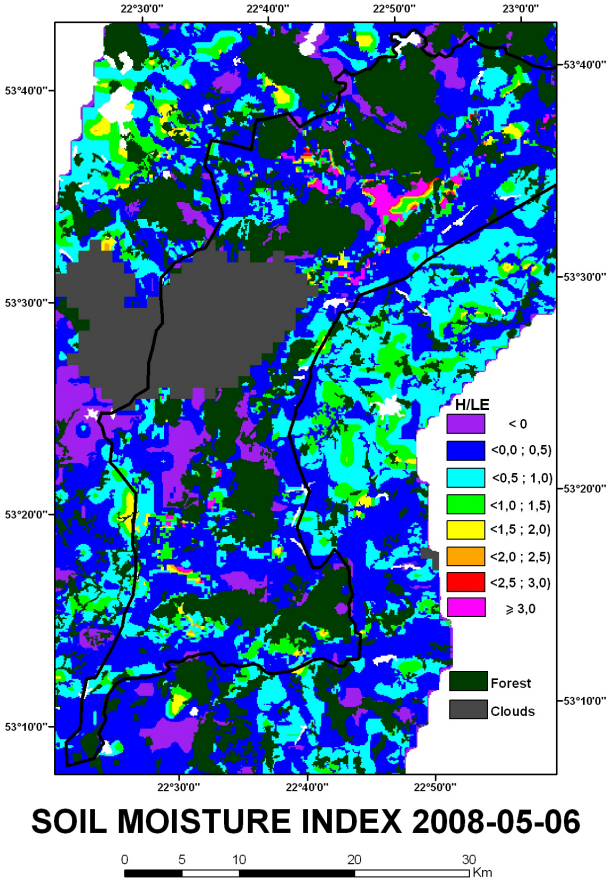

Fig. 7. SM index derived from NOAA.AVHRR.

HESSD
7, 5929–5955, 2010

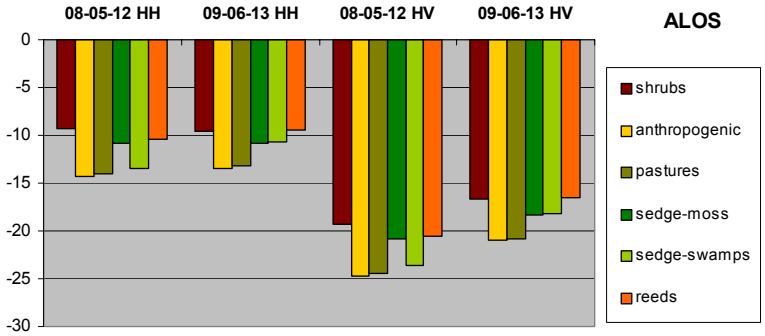

Fig. 8. Backscattering coefficient from ALOS.PALSAR data for classified communities.

HESSD
7, 5929–5955, 2010

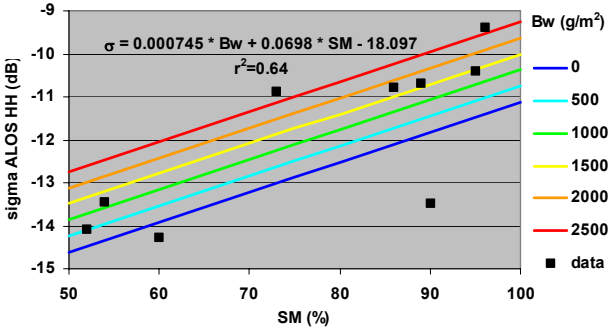

Fig. 9. Multicorrelation of biomass and soil moisture with backscatter ALOS.PALSAR HH.

HESSD
7, 5929–5955, 2010

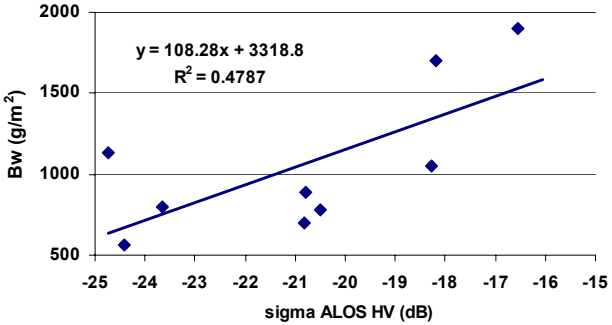

Fig. 10. Relationship of biomass and σ° from ALOS.PALSAR HV.

HESSD
7, 5929–5955, 2010

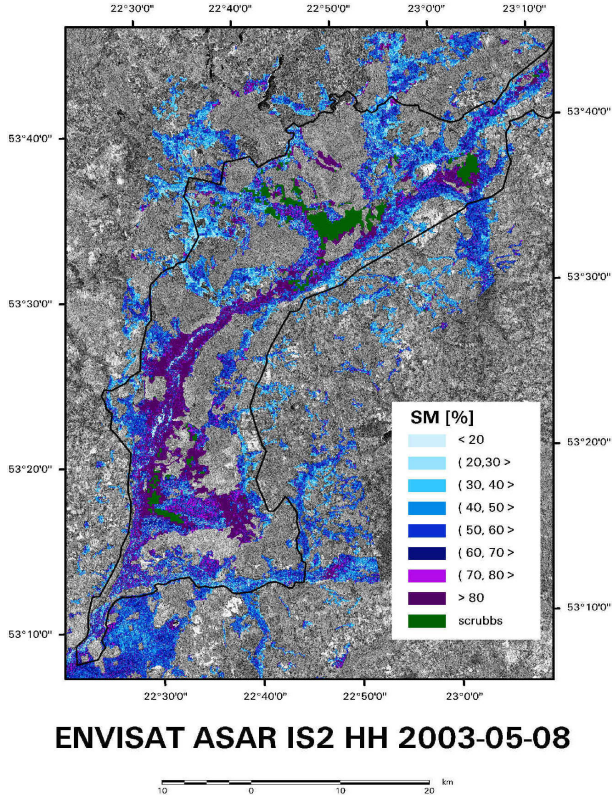

Fig. 11. Map of SM calculated from ASAR IS2 HH.

HESSD
7, 5929–5955, 2010

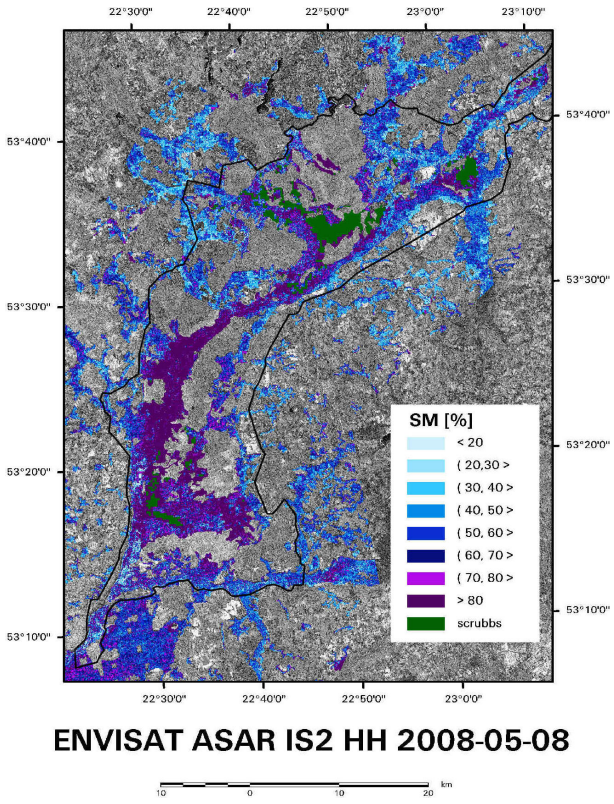

Fig. 12. Map of SM calculated from ASAR IS2 HH.

HESSD
7, 5929–5955, 2010

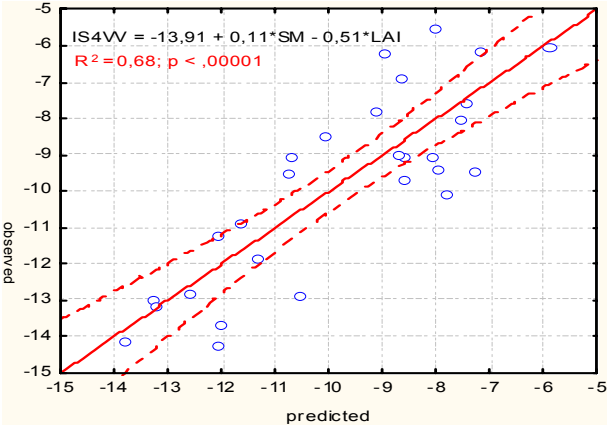

Fig. 13. Multiple regression between SM, LAI and σ° calculated from ASAR IS4 VV.

HESSD
7, 5929–5955, 2010

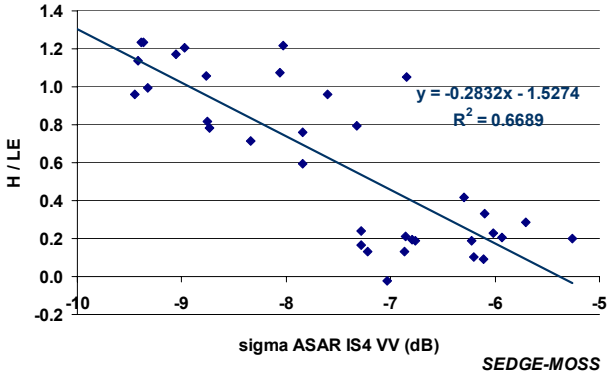

Fig. 14. Relationship between H/LE and σ° IS4 VV.

HESSD
7, 5929–5955, 2010